# THE MEASUREMENT OF BRANCHING RATIO OF $B_s^0 \to D_s^{\mp} K^{\pm}$ AND $B_s^0 \to D_s^- \pi^+$ IN THE LHCb EXPERIMENT*

Agnieszka Dziurda

on behalf of the LHCb Collaboration

The Henryk Niewodniczański Institute of Nuclear Physics
Polish Academy of Sciences
Radzikowskiego 152, 31-342 Kraków, Poland
and
Tadeusz Kościuszko Cracow University of Technology
Warszawska 24, 31-155 Kraków, Poland

*(Received May 5, 2012)*

The document reports the first observation of the $B_s^0 \to D_s^{\mp} K^{\pm}$ decays in the LHCb experiment together with the measurement of its branching fraction relative to the Cabibbo-favoured mode $B_s^0 \to D_s^- \pi^+$, $\frac{B(B_s^0 \to D_s^{\mp} K^{\pm})}{B(B_s^0 \to D_s^- \pi^+)}$ $= 0.0647 \pm 0.0044(\text{stat.})^{+0.0039}_{-0.0043}(\text{syst.})$. Furthermore, combining the yields obtained from 2010 data and the semileptonic LHCb measurements of the ratio of $b$-fragmentation fractions $f_s/f_d$, the branching fraction of the decay $B_s^0 \to D_s^- \pi^+$ is calculated, $B(B_s^0 \to D_s^- \pi^+) = (3.04 \pm 0.19(\text{stat.}) \pm 0.23(\text{syst.})^{+0.18}_{-0.16}(f_s/f_d))10^{-3}$. Finally, both measurements are used to obtain the absolute branching fraction of the $B_s^0 \to D_s^{\mp} K^{\pm}$ decay, $B(B_s^0 \to D_s^{\mp} K^{\pm}) = (1.97 \pm 0.18(\text{stat.})^{+0.19}_{-0.20}(\text{syst.})^{+0.11}_{-0.10}(f_s/f_d))10^{-4}$. The branching fraction measurements are significantly more precise than the existing world average values. The analysis is based on a 370 pb$^{-1}$ data sample collected in 2011 at LHC.

DOI:10.5506/APhysPolB.43.1483
PACS numbers: 13.25.Hw, 14.40.Nd

## 1. Introduction

The exploration of CP violation through studies of $B$-meson decays is at present one of the most important tasks of particle physics. In the Standard Model, CP violation is described by the presence of a single complex

* Presented at the Cracow Epiphany Conference on Present and Future of $B$ Physics, Cracow, Poland, January 9–11, 2012.

phase in the Cabibbo–Kobayashi–Maskawa mixing matrix [1]. The unitarity conditions of this matrix can be expressed in terms of the so-called a unitarity triangle. One of its angles, defined as $\gamma = \arg(-V_{ub}^* V_{ud}/V_{cb}^* V_{cd})$ can be determinated with negligible theoretical uncertainty through the study of time-dependent CP violation using $B_s^0 \to D_s^{\mp} K^{\pm}$ in the interference of decay and mixing [2]. The potential of the time-dependent $\gamma$ analysis can be understood based on a precise of determination of the branching ratio of the decay in question. In this analysis, the $B_s^0 \to D_s^{\mp} K^{\pm}$ branching fraction is measured relative to $B_s^0 \to D_s^- \pi^+$. The measurement of the $B_s^0$ and $B_0$ production fraction ratio $f_s/f_d$ is used to obtain the branching fraction of the decay $B_s^0 \to D_s^- \pi^+$. Finally, combining both results, the absolute branching fraction of $B_s^0 \to D_s^{\mp} K^{\pm}$ decay is found.

## 2. Event selection

The analysis is based on a data sample of 370 pb$^{-1}$ collected at the Large Hadron Collider (LHC) in 2011 at a centre-of-mass energy $\sqrt{s} = 7$ TeV. Because both considered decays are topologically identical, the event selection procedure is based mostly on topological information. However, in order to reject some specific backgrounds, PID requirements are also used (see Sec. 3). This procedure helps minimizing efficiency differences between the modes.

The LHCb detector [3] is a single-arm forward spectrometer covering the pseudo-rapidity range $2 < \eta < 5$. The detector includes a high precision tracking system consisting of a silicon-strip vertex detector, a large-area silicon-strip detector located upstream of a dipole magnet with a bending power of about 4 Tm, and three stations of silicon-strip detectors and straw drift tubes placed downstream. The combined tracking system has a momentum resolution $\Delta p/p$ that varies from 0.4% at 5 GeV/$c$ to 0.6% at 100 GeV/$c$. Two ring-imaging Cherenkov detectors (RICH) are used to identify charged particles. Photon, electron and hadron candidates are identified by a calorimeter system consisting of scintillating-pad and pre-shower detectors, an electromagnetic calorimeter and a hadronic calorimeter. Muons are identified by alternating layers of iron and multiwire proportional chambers.

The first stage of event selection is the LHCb trigger, composed of two steps. The initial, hardware trigger is based on information from the calorimeter and muon systems, followed by a software stage which applies a full event reconstruction. Here, only two subsamples are considered: so-called triggered on the signal (TOS) events which pass the hadronic first-level trigger exclusively on signal and not on the rest of the event; and events triggered independently of signal (TIS). Events not entering either of these two exclusive categories are discarded. At the second software stage a two-,

three-, or four-track secondary vertex with a high sum of the transverse momenta ($p_{\mathrm{T}}$) of the tracks and significant displacement from the primary interaction is required. In addition one of tracks has to satisfy the conditions:

- $p_{\mathrm{T}} > 1.7\,\mathrm{GeV}/c^2$,
- impact parameter $\chi^2 > 16$,
- track fit $\chi^2$ per degree of freedom of the fit $\chi^2/\mathrm{ndf} < 2$.

The events which pass the trigger are considered in the preselection stage. The $D_s^-$ meson is reconstructed from two kaons with opposite charge, and a pion. Then $B_s^0$ candidates are reconstructed from a selected $D_s^-$ candidate and, depending on the mode, a pion or kaon. The selection criteria are optimized to reject background using conditions:

- well-reconstructed tracks for all particles:
  - — track $\chi^2/\mathrm{ndf} < 4$,
  - — high transverse momentum with respect to the primary vertex,
  - — large impact parameter with respect to the primary vertex,
- in order to remove charmless background: the flight distance $\chi^2$ of the $D_s^-$ from the $B_s^0 > 2$,
- vertex fit $\chi^2/\mathrm{ndf} < 9$ for $D_s^-$ and $B_s^0$ mesons,
- $\cos(\theta_{\mathrm{flight}}) > 0.9999$, where $\theta_{\mathrm{flight}}$ is the angle between the $B_s^0$ momentum vector and its direction of flight,
- $\chi^2$ of impact parameter w.r.t. the primary vertex $< 16$ for $B_s^0$ meson.

A gradient boosted decision tree (BDTG) [4] is used in the last offline stage of event selection. The optimal working point is chosen by evaluating the signal significance with respect to the combinatoric background

$$\mathrm{Sig}_{D_s K} = \frac{S/14}{\sqrt{S/14 + B}}\,, \tag{1}$$

where S and B denote the number of reconstructed signal and background events in the $B_s^0$ mass window. The factor 14 is chosen because of the expected reduction of yield for the Cabibbo suppressed mode. In order to avoid biases in the result, only 10% of the full data sample is used in this optimization. At the optimal BDTG value of 0.1 a signal significance of 4.4 is obtained corresponding to a reduction of the signal yield of 6% with a background reduction of 45%.

## 3. Particle identification

All PID criteria are based on the difference in log-likelihood between kaon and proton or pion hypotheses, DLL($K-p$) and DLL($K-\pi$). The efficiency and misidentification probabilities for the PID criteria are summarized in Table I.

In particular, DLL($K-\pi$) $< 0$ and DLL($K-\pi$) $> 5$ are required in order to separate the Cabibbo favoured $B_s^0 \to D_s^- \pi^+$ mode from the suppressed $B_s^0 \to D_s^\mp K^\pm$ mode.

Further background rejection is obtained using the PID criteria for $D_s$ children. The sizeable $B^0 \to D^- \pi^+$ background is suppressed by requiring that the kaon with the same charge as the pion have a DLL($K-\pi$) $> 5$. Moreover, the other kaon is required to satisfy DLL($K-\pi$) $> 0$ and the pion DLL($K-\pi$) $< 5$.

In order to suppress the $\overline{\Lambda}_b^0 \to \overline{\Lambda}_c^- \pi^+$ contribution, two steps are applied and at least one of them has to be satisfied. First of all, the requirement DLL($K-p$) $> 5$ for the kaon with the same charge as the pion is invoked. Secondly, the candidate is reconstructed under $\overline{\Lambda}_c^- \to \overline{p} K^+ \pi^-$ mass hypotheses and is accepted if it does not fall into the $\overline{\Lambda}_c^-$ signal mass window. The latter is defined as $\pm 25\,\mathrm{MeV}/c^2$ around the nominal value of $2285\,\mathrm{MeV}/c^2$ [5].

TABLE I

Efficiency and misidentification probabilities, split by magnet polarity, for the bachelor PID cuts used in the analysis. Probabilities are obtained from the efficiencies in the $D^*$ calibration sample, binned in momentum and $p_\mathrm{T}$. Only bachelor tracks with momentum below 100 GeV/$c$ are considered. The error shown is the statistical error due to the finite number of signal events used in the reweighting.

| | PID Cut | Efficiency | |
|---|---|---|---|
| | | Magn. down | Magn. up |
| $K$ | DLL($K-\pi$) $> 5$ | $83.5 \pm 0.2\%$ | $83.3 \pm 0.2\%$ |
| $\pi$ | DLL($K-\pi$) $< 0$ | $85.8 \pm 0.2\%$ | $84.2 \pm 0.2\%$ |
| | | MisID | |
| | | Magn. down | Magn. up |
| $K$ | DLL($K-\pi$) $> 5$ | $4.5 \pm 0.1\%$ | $5.3 \pm 0.1\%$ |
| $\pi$ | DLL($K-\pi$) $< 0$ | $5.4 \pm 0.1\%$ | $5.3 \pm 0.1\%$ |

## 4. Mass fits

The mass fits require the determination of signal and background parametrizations. The simulated signal events with the full event selection chain are used to determinate the signal lineshapes. Various lineshape

parametrizations have been examined and the best fit is obtained using a double Crystall Ball function with power-law tails or opposite sides. The $D_s$ meson mass is constrained to its PDG [5] value in order to improve the $B_s^0$ mass resolution. Three background contributions need to be considered: fully reconstructed misidentified backgrounds, partially reconstructed backgrounds with or without misidentification and combinatorial backgrounds.

The most significant fully reconstructed backgrounds for $B_s^0 \to D_s^{\mp} K^{\pm}$ are those due to $B^0 \to D_s^{\mp} K^{\pm}$ and $B_s^0 \to D_s^- \pi^+$, whereas for $B_s^0 \to D_s^- \pi^+$ the most significant background is $B^0 \to D^- \pi^+$. In the case of $B^0 \to D_s^{\mp} K^{\pm}$ the shape of the signal is fixed to be the same as for $B_s^0 \to D_s^{\mp} K^{\pm}$, but the mean is floated in the fit. That mode is reconstructed under its own mass hypothesis. The parametrization of the remaining contribution of fully reconstructed background is obtained from a reweighting procedure. The mass shapes under the wrong mass hypothesis depend on the momentum distribution of the misidentified particle. This momentum distribution must, therefore, be reweighted by taking into account the momentum dependence on the misID rate. This dependence is obtained using a dedicated calibration sample of prompt $D^{*+}$ decays. The mass distributions under the wrong mass hypothesis are then reweighted using this momentum distribution to obtain the $B^0 \to D^- \pi^+$ and $B_s^0 \to D_s^- \pi^+$ mass shapes under the $B_s^0 \to D_s^- \pi^+$ and $B_s^0 \to D_s^{\mp} K^{\pm}$ mass hypotheses, respectively.

The mass templates for partially reconstructed backgrounds are taken from samples of simulated events generated in specific exclusive modes, corrected for the observed mass shifts, momentum spectra, and particle identification efficiencies observed in data. The use of simulated events is justified by the observed good agreement between data and simulation.

The parametrization of the combinatorial background depends on considered decay mode. For the $B_s^0 \to D_s^- \pi^+$ and $B^0 \to D^- \pi^+$ it is described as an exponential function with floating parameter. For the $B_s^0 \to D_s^{\mp} K^{\pm}$ the parametrization is taken from wrong side events and is fixed to be flat, because of the partially reconstructed backgrounds which dominate in the mass region below the signal peak.

In $B_s^0 \to D_s^{\mp} K^{\pm}$ there are also present the contributions from $\Lambda_b^0 \to D_s^- p$ and $\Lambda_b^0 \to D_s^{*-} p$ modes. Due to the fact that the decays $B^0 \to D^- D_s^+$ and $B^0 \to D^- D_s^{*+}$ have almost equal branching fraction it is assumed that $\Lambda_b^0 \to D_s^- p$ and $\Lambda_b \to D_s^{*-} p$ have equal weights in the fit. The shapes of parametrizations are taken from simulated data with application of the reweighting procedure for PID criteria $\mathrm{DLL}(K-p) > 5$, however the $\Lambda_b^0 \to D_s^{*-} p$ shape is shifted $200\,\mathrm{MeV}/c^2$ downward.

The extended maximum likelihood fits is used to obtain the signal yields. The magnet up and down data are considered separately in order to achieve the highest sensitivity.

The mass fits to the $B_s^0 \to D_s^- \pi^+$ hypothesis are presented in Fig. 1 and the fit results are summarized in Table II. The free parameters in the fit are: the mean and yield of the signal, the yields of the different partially reconstructed backgrounds (except $B^0 \to D^- \pi^+$) and the shape of the combinatoric background. The lineshape of $B^0 \to D^- \pi^+$ mass distribution is taken from an additional, separate fit. The yield ratio between $B_s^0 \to D_s^- \pi^+$ and $B^0 \to D^- \pi^+$ is fixed to the computed value of $1/35$ in each fit for the two polarities, taking into account the PDG branching fractions and the measured LHCb value of $f_s/f_d$. The contribution expected from $B^0 \to D^- \pi^+$ has a 10% uncertainty assigned to it, accounting for particle misidentification efficiencies. The yield of $\overline{\Lambda}_b^0 \to \overline{\Lambda}_c^- \pi^+$ is a free parameter of the fit and is found to be consistent with zero.

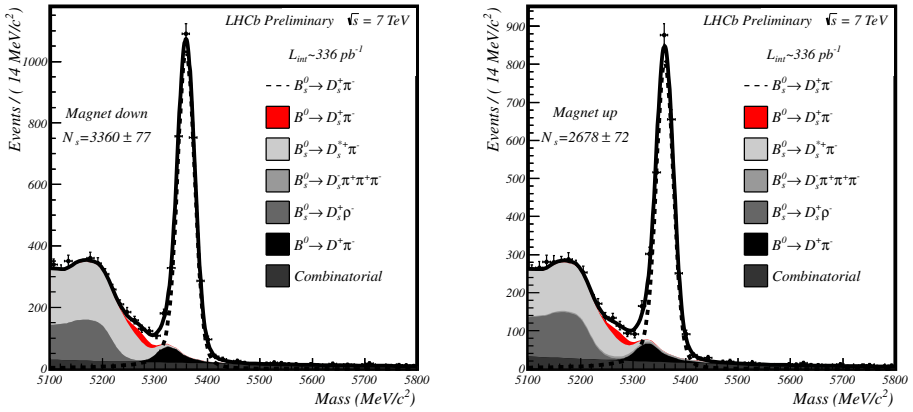


Fig. 1. Fit to the $B_s^0 \to D_s^- \pi^+$ candidates, split per magnet polarity.

TABLE II

Results of the fit to the data $B_s^0 \to D_s^- \pi^+$ candidates.

| Parameter | Fit value | |
|---|---|---|
| | Magn. down | Magn. up |
| Num. combinatorics | $860 \pm 150$ | $790 \pm 230$ |
| Num. part. reco. | $3200 \pm 100$ | $2420 \pm 120$ |
| Num. $B_s^0 \to D_s^- \pi^+$ | $3360 \pm 77$ | $2678 \pm 72$ |
| $B_s^0 \to D_s^- \pi^+$ mass mean [MeV/$c^2$] | $5359.4 \pm 0.4$ | $5360.4 \pm 0.5$ |

The fits to the $B_s^0 \to D_s^{\mp} K^{\pm}$ hypothesis are shown in Fig. 2, whereas Table III collects the fit results. The signal mass region has numerous contaminations from other decays. The model is more complicated because of the presence of many reflections which have relatively similar mass shapes. The most important reflection is due to $B_s^0 \to D_s^- \pi^+$. Its shape is taken

from real data all selection cut applied as for $B_s^0 \to D_s^{\mp} K^{\pm}$, except for the bachelor PID requirement, and reweighted according to the PID cuts. The information on PID efficiency is used to constrain the number of events in the $B^0 \to D^- K^+$ mode and is found to be 16 (17) events for up (down) polarity. Furthermore, there is a possible cross-feed from partially reconstructed modes with a misidentified pion such as $B_s^0 \to D_s^- \rho^+$. For this reason, based on on criteria such as relative branching fractions, reconstruction efficiencies and (mis-)identification probabilities, the yields of those modes whose branching fractions are known or can be estimated are constrained. All the constrained yields are collected in Table III. An important cross-check is performed by comparing the fitted value of the $B_s^0 \to D_s^- \pi^+$ signal yield to the expected yield. The expected numbers are: $188 \pm 8$ events in the magnet down sample, and $182 \pm 8$ events in the magnet up sample. Comparing to the observed event yields both of the expected numbers are approximately $1\sigma$ high.

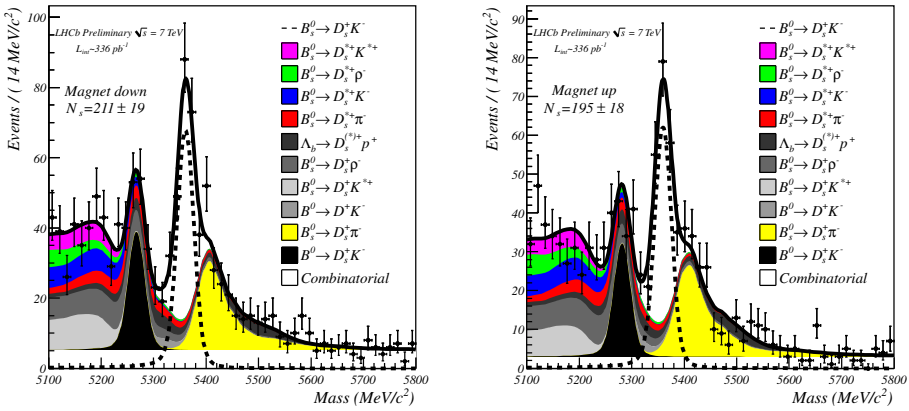


Fig. 2. Fit to the $B_s^0 \to D_s^{\mp} K^{\pm}$ candidates, split per magnet polarity.

TABLE III

Results of the fit to the $B_s^0 \to D_s^{\mp} K^{\pm}$ candidates. The number quoted for $B_s^0 \to D_s^- \pi^+$ also includes a small (around 20 events from the misID expectation) quantity of $B^0 \to D^- \pi^+$ events which are not fitted for separately, as they have a similar mass shape. For the constrained signals the reader is referred to Table IV.

| Parameter | Fit value | |
|---|---|---|
| | Magn. down | Magn. up |
| Num. $B^0 \to D_s^{\mp} K^{\pm}$ | $105 \pm 18$ | $91 \pm 17$ |
| Num. $B_s^0 \to D_s^- \pi^+$ and $B^0 \to D^- \pi^+$ | $161 \pm 22$ | $158 \pm 21$ |
| Num. $B_s^0 \to D_s^{\mp} K^{\pm}$ | $211 \pm 19$ | $195 \pm 18$ |
| $B_s^0 \to D_s^{\mp} K^{\pm}$ mass mean [MeV/$c^2$] | $5360.8 \pm 1.8$ | $5359.7 \pm 1.8$ |

TABLE IV

Gaussian constraints applied in the $B_s^0 \to D_s^{\mp} K^{\pm}$ fit to the partially reconstructed or misidentified backgrounds.

| Background type | Magn. down | Magn. up |
|---|---|---|
| $B_s^0 \to D_s^{*-}\pi^+$ | $70 \pm 23$ | $63 \pm 21$ |
| $B_s^0 \to D_s^{*-}K^+$ | $80 \pm 27$ | $72 \pm 34$ |
| $B_s^0 \to D_s^{-}\rho^+$ | $150 \pm 50$ | $135 \pm 45$ |
| $B_s^0 \to D_s^{-}K^{*+}$ | $150 \pm 50$ | $135 \pm 45$ |
| $B_s^0 \to D_s^{*-}\rho^+$ | $50 \pm 17$ | $45 \pm 15$ |
| $B_s^0 \to D_s^{*-}K^{*+}$ | $50 \pm 17$ | $45 \pm 15$ |
| $\Lambda_b \to D_s^{-}p$ and $\Lambda_b \to D_s^{*-}p$ | $80 \pm 27$ | $72 \pm 34$ |

## 5. Systematic uncertainties

The systematic uncertainties on the measurement of the relative branching fraction of $B_s^0 \to D_s^{\mp} K^{\pm}$ and $B_s^0 \to D_s^{-}\pi^+$ are related to the fit model, particle identification calibration, and trigger and offline selection efficiency corrections. The total systematics budget is listed in Table V.

TABLE V

The final systematics budget for the measurement of the branching fraction of $B_s^0 \to D_s^{\mp} K^{\pm}$ relative to $B_s^0 \to D_s^{-}\pi^+$. In the case of the generator and non-PID selection efficiencies, taken from simulated events, the full size of the efficiency correction is assigned as a systematic uncertainty.

| Source | Uncertainty |
|---|---|
| Generator Efficiency | 3% |
| All non-PID selection | 3% |
| Fit model $B_s^0 \to D_s^{-}\pi^+$ | 0.9% |
| Fit model $B_s^0 \to D_s^{\mp} K^{\pm}$ | +4%, −5% |
| PID selection | 0.9% |
| Total | +5.9%, −6.7% |

The systematic uncertainty in the fit model is related to the parameters. In the first considered fit model, $B_s^0 \to D_s^{-}\pi^+$, the uncertainty comes from the $B^0 \to D_s^{-}\pi^+$ yield and the widths and Crystal Ball tail values of the signal which are fixed from simulation. The final $B_s^0 \to D_s^{-}\pi^+$ fit systematic uncertainty is found to be 0.9%.

The systematic uncertainties on the $B_s^0 \to D_s^{\mp} K^{\pm}$ fit are more involved because of the treatment of partially reconstructed backgrounds. The following source of systematic uncertainties are considered: fixing parameters in the lineshapes, the combinatorial background shapes, the partially recon-

structed backgrounds taking into account their contribution to the signal mass region. Due to fact that the combinatoric background cannot very well rise with mass, its uncertainty is taken as asymmetric. Moreover, the uncertainties from $\Lambda_b^0 \to D_s^- p$ and $\Lambda_b^0 \to D_s^{*-} p$ are assumed to contribute equally. Adding these effects in quadrature, an overall systematic uncertainty of $+4\%$ and $-5\%$ is assigned.

Two kinds of sources of PID uncertainties are considered. Firstly, the overall efficiencies and misidentification probabilities are taken into account. The second part comes from the fit model, where the misidentified backgrounds are included using reweighing of PID efficiency *versus* momentum. The systematic uncertainties from that source is found to be 0.9%.

The observed ratio of $B_s^0 \to D_s^{\mp} K^{\pm}$ and $B_s^0 \to D_s^- \pi^+$ events needs to be corrected for efficiency differences, beginning with the kinematic/geometric selection chain of trigger-preselection-offline selection. The efficiencies are measured using Monte Carlo MC10 simulated events which have had the 2011 trigger run on them. One would expect the efficiency ratio to be close to, but not precisely unity due to the differences in lifetimes of the $K^{\pm}$ and $\pi^{\pm}$, and the different interactions in the detector material. The ratio of efficiency is found to be $\epsilon_{B_s^0 \to D_s^{\mp} K^{\pm}} / \epsilon_{B_s^0 \to D_s^- \pi^+} = 1.058 \pm 0.014$. For that reason, an additional 3% of systematic uncertainty is taken.

## 6. Extraction of the branching fractions

The $B_s^0 \to D_s^{\mp} K^{\pm}$ branching fraction relative to $B_s^0 \to D_s^- \pi^+$ can be determinated based on the raw signal yields for PID and selection efficiency differences

$$\frac{B\left(B_s^0 \to D_s^{\mp} K^{\pm}\right)}{B\left(B_s^0 \to D_s^- \pi^+\right)} = \frac{N_{B_s^0 \to D_s^{\mp} K^{\pm}}}{N_{B_s^0 \to D_s^- \pi^+}} \frac{\epsilon^{\mathrm{PID}}_{B_s^0 \to D_s^- \pi^+}}{\epsilon^{\mathrm{PID}}_{B_s^0 \to D_s^{\mp} K^{\pm}}} \frac{\epsilon^{\mathrm{Sel}}_{B_s^0 \to D_s^- \pi^+}}{\epsilon^{\mathrm{Sel}}_{B_s^0 \to D_s^{\mp} K^{\pm}}}, \tag{2}$$

where $N_{B_s^0 \to D_s^{\mp} K^{\pm}} = 406 \pm 26$, $N_{B_s^0 \to D_s^- \pi^+} = 6038 \pm 105$, $\epsilon^{\mathrm{PID}}_{B_s^0 \to D_s^{\mp} K^{\pm}} = 83.4 \pm 0.2$, $\epsilon^{\mathrm{PID}}_{B_s^0 \to D_s^- \pi^+} = 85.0 \pm 0.2$, and the ratio of the two selection efficiencies is $0.945 \pm 0.013$. The ratio of branching fractions is found to be

$$\frac{B\left(B_s^0 \to D_s^{\mp} K^{\pm}\right)}{B\left(B_s^0 \to D_s^- \pi^+\right)} = 0.0647 \pm 0.0044\ (\mathrm{stat.})\ {}^{+0.0039}_{-0.0043}\ (\mathrm{syst.})\,. \tag{3}$$

Combining this result with the measurement of $f_s/f_d$ based on semileptonic decays, described in Ref. [7], and the yields measured in Ref. [6] the

absolute branching fraction of $B_s^0 \to D_s^- \pi^+$ is extracted

$$B\left(B_s^0 \to D_s^- \pi^+\right) = B\left(B^0 \to D^- \pi^+\right) \times \frac{\epsilon_{B^0 \to D^- \pi^+}}{\epsilon_{B_s^0 \to D_s^- \pi^+}} \frac{N_{B_s^0 \to D_s^- \pi^+} B(D^+ \to K^- \pi^+ \pi^+)}{\frac{f_s}{f_d} N_{B^0 \to D^- \pi^+} B(D_s^+ \to K^+ K^- \pi^+)}, \quad (4)$$

where $\epsilon_X$ is the efficiency to reconstruct decay modes $X$ and $N_X$ is the number of observed events in this decay mode. Using input collected in Table VI the $B_s^0 \to D_s^- \pi^+$ branching fraction is obtained

$$B(B_s^0 \to D_s^- \pi^+) = \left(3.04 \pm 0.19\ (\text{stat.}) \pm 0.23\ (\text{syst.})\ ^{+0.18}_{-0.16}\ (f_s/f_d)\right) \times 10^{-3}, \quad (5)$$

where the first uncertainty is statistical, the second the systematic uncertainty arising from external factors (the $B^0$, $D_s^-$, and $D^-$ branching fractions), and the third one is the additional asymmetric systematic uncertainty from the semileptonic $f_s/f_d$ measurement, as well as experimental systematics on the ratio of $B_s^0 \to D_s^- \pi^+$ and $B^0 \to D^- \pi^+$ events.

TABLE VI

Numbers entering the calculation of the branching fraction of $B_s^0 \to D_s^- \pi^+$, taken from [6, 7, 8] and reproduced for the reader's convenience.

| Parameter | Value |
|---|---|
| $B(B^0 \to D^- \pi^+)$ | $(2.68 \pm 0.13) \times 10^{-3}$ |
| $B(D^+ \to K^- \pi^+ \pi^+)$ | $(9.14 \pm 0.20) \times 10^{-2}$ |
| $B(D_s^+ \to K^+ K^- \pi^+)$ | $(5.49 \pm 0.27) \times 10^{-2}$ |
| $N_{B_s^0 \to D_s^- \pi^+}$ | $670 \pm 34$ |
| $N_{B^0 \to D^- \pi^+}$ | $4103 \pm 75$ |
| $\epsilon_{B^0 \to D^- \pi^+}/\epsilon_{B_s^0 \to D_s^- \pi^+}$ | $1.120 \pm 0.025$ |
| Fit Model systematic | 2.8% |
| PID systematic | 2.0% |
| Trigger systematic | 2.0% |
| $f_s/f_d$ | $0.268 \pm 0.008(\text{stat.})^{+0.022}_{-0.020}(\text{syst.})$ |

Finally, based on the results from Eq. (3) and Eq. (5) the absolute branching fraction of $B_s^0 \to D_s^\mp K^\pm$ is determined

$$B\left(B_s^0 \to D_s^\mp K^\pm\right) = \left(1.97 \pm 0.18\ (\text{stat.})\ ^{+0.19}_{-0.20}\ (\text{syst.})\ ^{+0.11}_{-0.10}\ (f_s/f_d)\right) \times 10^{-4}, \quad (6)$$

where the first uncertainty is statistical, the second reflects experimental systematics, and the third arises from knowledge of $f_s/f_d$.

## 7. Summary

The document presents the results from LHCb experiment based on $370\,\mathrm{pb}^{-1}$ data collected at LHC in 2011. The analysis considered the $B^0_{d,s} \to D^-_{(s)} h^+$ family of modes. The branching fraction $B_s^0 \to D_s^{\mp} K^{\pm}$ relative to the Cabibbo-favoured mode $B_s^0 \to D_s^- \pi^+$ is found: $\frac{B(B_s^0 \to D_s^{\mp} K^{\pm})}{B(B_s^0 \to D_s^- \pi^+)} = 0.0647 \pm 0.0044(\mathrm{stat.}) \pm^{+0.0039}_{-0.0043} (\mathrm{syst.})$. Based on the the semileptonic LHCb measurements of the ratio of $b$-fragmentation fractions $f_s/f_d$ and the yield obtained from 2010 data, the branching fraction of the decay $B_s^0 \to D_s^- \pi^+$ is calculated, $B(B_s^0 \to D_s^- \pi^+) = (3.04 \pm 0.19(\mathrm{stat.}) \pm 0.23(\mathrm{syst.})^{+0.18}_{-0.16}(f_s/f_d))10^{-3}$. Finally, the absolute branching fraction of $B_s^0 \to D_s^{\mp} K^{\pm}$ decay is obtained: $B(B_s^0 \to D_s^{\mp} K^{\pm}) = (1.97 \pm 0.18(\mathrm{stat.})^{+019}_{-0:20}(\mathrm{syst.})^{+0.11}_{-0.10}(f_s/f_d))10^{-4}$.

## REFERENCES


[1] M. Kobayashi, T. Maskawa, *Prog. Theor. Phys.* **49**, 652 (1973).

[2] R. Fleischer, *Nucl. Phys.* **B671**, 459 (2003) [arXiv:hep-ph/0304027v2].

[3] A.A. Alves Jr. *et al.* [LHCb Collaboration], *JINST* **3**, S08005 (2008).

[4] A. Hocker *et al.*, *PoS* **ACAT**, 040 (2007) [arXiv:physics/0703039v5 [physics.data-an]].

[5] http://pdg.lbl.gov/

[6] R. Aaij *et al.* [LHCb Collaboration], *Phys. Rev. Lett.* **107**, 211801 (2011) [arXiv:1106.4435v2 [hep-ex]].

[7] R. Aaij *et al.* [LHCb Collaboration], Tech. Rep. LHCb-CONF-2011-028, Jun 2011.

[8] R. Aaij *et al.* [LHCb Collaboration], Tech. Rep. LHCb-CONF-2011-034, Jul 2011.